Learning Based Single Frame Image Super-resolution Using Fast Discrete Curvelet Coefficients

Anil A. Patil *panil21mail@gmail.com*
Department of Electronics & Telecommunication
COE, Malegaon(Bk),
Pune, India.

Jyoti Singhai *j.singhai@gmail.com*
Department of Electronics & Communication Engg.
MANIT, Bhopal,India.

Abstract

High-resolution (HR) images play a vital role in all imaging applications as they offer more details. The images captured by the camera system are of degraded quality due to the imaging system and are low-resolution (LR) images. Image super-resolution (SR) is a process, where HR image is obtained from combining one or multiple LR images of same scene. In this paper, learning based single frame image super-resolution technique is proposed by using Fast Discrete Curvelet Transform (FDCT) coefficients. FDCT is an extension to Cartesian wavelets having anisotropic scaling with many directions and positions, which forms tight wedges. Such wedges allow FDCT to capture the smooth curves and fine edges at multiresolution level. The finer scale curvelet coefficients of LR image are learnt locally from a set of high-resolution training images. The super-resolved image is reconstructed by inverse Fast Discrete Curvelet Transform (IFDCT). This technique represents fine edges of reconstructed HR image by extrapolating the FDCT coefficients from the high-resolution training images. Experimentation based results show appropriate improvements in MSE and PSNR.

Keywords: Super-resolution, Multiresolution, Learning Method, Fast Discrete Curvelet Transform

1. INTRODUCTION

High resolution (HR) images are essential in almost all imaging applications. HR images provide additional details that are essential, to the success of various applications that require accurate image analysis such as image/video resolution enhancement, medical imaging, remote sensing and video surveillance, etc. The image captured by current camera system is of degraded quality because of the resolution of a digital imaging device which is mainly limited by the number of pixels on the sensor and the optical system. Such captured images are acknowledged as low-resolution images (LR). The spatial resolution of the low resolution image can be improved by increasing the pixel density or by growing the chip-size. Both techniques enforce certain limitations. The spatial resolution of a single image (frame) can be enhanced by the traditional interpolation techniques. It has also limited application since aliasing is present. The inherent limitations of the current camera system are prevailed over by the technique known as Super-resolution (SR) based on digital signal processing. SR is a technique where one or many low resolution images (frames) are combined to obtain a high spatial resolution image. In this process low resolution image is upsampled by recovering the missing high frequency details and degradations are impassive. Super-resolution reconstruction technique is basically classified in two categories as reconstruction based and learning based methods. In reconstruction based methods high–resolution image is obtained from several low-resolution observations by proper fusion of a series of accurately registered aliased images. Most of the literature available on super-resolution is for multi-frame and majority of them are based on the motion as cue. The super-resolution idea was introduced by Tsai and Hung, where a pure translation motion has been considered [1]. In such methods the quality of reconstructed SR image obtained from a set

of LR images depends upon the registration accuracy of the LR images and some prior knowledge of imaging system [2, 3]. The ideal sub-pixel displacement errors in the observation with noise can be used to obtain a high resolution image by constrained total least square algorithm [4] and their effect on the convergence rate of iterative approach is discussed by Ng and Bose [5]. All these iterative methods are computationally complex. In many resolution enhancement applications the point spread function (PSF) of the imaging system is unknown which reflects in blur. Nguyen et al. propose a technique for parametric blur identification and regularization based on generalized cross-validation (GVC) theory where circulant block preconditioners are used to accelerate the conjugate gradient decent (CG) method for solving the Tikhonor-regularization super-resolution problem [6]. Single observed image expansion by interpolation or super-resolution smooth the image data at edge regions. A maximum a posteriori (MAP) estimator with Huber-Markove random field (MRF) prior can be used for image expansion [7]. In recent work blur, defocus, zoom are used as cues for super-resolving the low resolution image [8, 9]. The SR image problem can be solved by combining, maximum likelihood (ML) estimator, MAP estimator and projection onto convex sets (POCS) to find unified approach [10].
Learning methods becomes more useful, when only a single observation is available and several other high resolution images are present in the data set. All high resolution images from data set will act as training images. In many realistic applications, such as in biometry, criminal surveillance a single observation is available. Nearly all SR reconstruction algorithms are based on the fundamental constraints that provide less useful information as the magnification factor increases. Baker and Kanade found these limitations and developed a SR algorithm by modifying the prior term in cost to include the result of a set of recognition called as recognition based super-resolution or hallucination [11]. A similar approach is used for multiple views using learned image models through use of principal component analysis (PCA) Capel and Zisserman [12]. A fast and simple one pass example based super-resolution algorithm is proposed by Freeman et al. which is resolution independent [13]. Zoomed observations have been used to reconstruct super-resolved image by learning the high resolution image model through most zoomed observations [14]. In SR, handling of data at different resolution level is tedious. The multiresolution technique can handle data well. In wavelet transform based learning technique high frequency coefficients of the unknown high-resolution image are learned locally from a set of training images based on best match by Jiji et al. [15]. Chang et. al. have proposed method where the generation of the high resolution image patch depends simultaneously on multiple nearest neighbors in the training set [16]. Face is represented by linear combination of prototypes of shapes and texture in top-down learning of LR facial images by Park and Lee [17]. An image hallucination approach based on primal sketch prior with reconstruction constraint to improve the quality is proposed by Sun et al. [18]. Multiscale, directional Contourlet transform is proposed by M.N.Do and M.Vetterli. It decomposes image in scales with directional subbands thus captures the smoothness along the contours [19]. Jiji and Chaudhuri have proposed a single frame image super-resolution through Contourlet learning which learns the best edge primitives from the HR training set in contourlet domain [20]. Recently a frame work to combine power of reconstruction and learning based methods is proposed, where redundancy within single image is used. It requires registration at subpixel accuracy and is computationally complex [24]. New learning based SR technique using DWT and IGMRF prior improves the quality of reconstructed image [23]. By introducing the statistics to learning-based super-resolution with global and local constraints to obtain high quality reconstructed image is proposed by Kim et al. [25]. A SR problem can be resolved by kernel ridge regression (KRR) with a prior model of a generic image class is suggested by Kim and Kown [26]. In this paper a geometric curvelet transform (FDCT) [21, 22] is proposed to learn the salient features from the data set while upsampling the input image. FDCT gives sparse representation of C^2 function away from edges along piecewise smooth curves. The super-resolved image represents the learnt features of low resolution oriented edges from the high resolution data set. This leads to significant improvement in quality of the reconstructed image.

This paper is organized as follows: imaging model is shown in section 2. Section 3 discusses the Fast discrete curvelet transform. Procedure to learn the fast discrete curvelet coefficients is

discussed in section 4. Experimentation results on different gray and color images are discussed in section 5. Paper concludes with section 6.

2. THE IMAGING MODEL

In this paper, the following linear image formation model is adapted to obtain observed low resolution image.

$$y = DBx + n \tag{1}$$

where x is a original high resolution image represented lexicographically ordered of $M^2 \times 1$ pixel size, D is decimation matrix and B is the blur matrix. The size of the decimation matrix depends upon the decimation factor and is not invertible. y is a low resolution observation obtained, and represented lexicographically in order of $N^2 \times 1$ pixel size and n is noise vector of size $M^2 \times 1$. Here noise is assumed to be zero mean independent identically distributed and blur to be an identity matrix. For a single observation y, high resolution image x is estimated. The imaging model is illustrated in Figure 1.

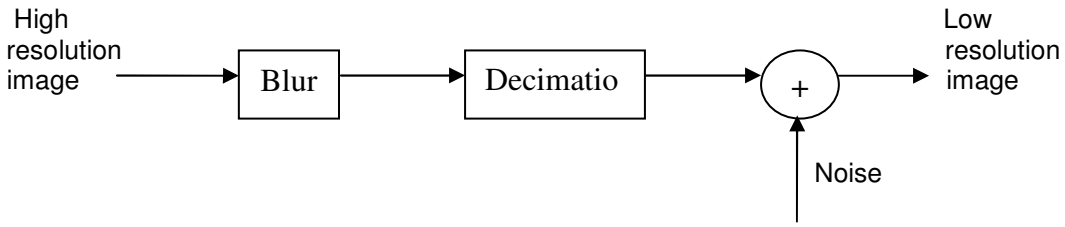

FIGURE 1: Illustration of low-resolution image formation model

3. FAST DISCRETE CURVELET TRANSFORM

Fast Discrete Curvelet transform (FDCT) gives local components at different frequencies for analysis and synthesis of digital image in multi-resolution analysis. FDCT is multi-scale geometric transform, which is a multi-scale pyramid with many directions and positions at each length scale. FDCT is basically 2D anisotropic extension to classical wavelet transform that has main direction associated with it. Analogous to wavelet, FDCT can be translated and dilated. The dilation is given by a scale index that controls the frequency content of the curvelet with the indexed position and direction can be changed through a rotation. This rotation is indexed by an angular index. Curvelet satisfy anisotropic scaling relation, which is generally referred as parabolic scaling. This anisotropic scaling relation associated with FDCT is a key ingredient to the proof that curvelet provides sparse representation of the C^2 function away from edges along piecewise smooth curves. FDCT is constructed by a radial window W and angular window V. The radial window W is expressed as

$$\tilde{W}_j(w) = \sqrt{\phi_{j+1}^2(w) - \phi_j^2(w)} \quad , \quad j \geq 0 \tag{2}$$

Where, j is scale and ϕ is defined as the product of low-pass one dimensional window and separate scales in Cartesian equivalents. The angular window V is defined as

$$V_j(w) = V\left(2^{\lfloor j/2 \rfloor} w_2 / w_1\right) \tag{3}$$

where, $W1$ and $W2$ are low pass one dimensional windows. The Cartesian window $\tilde{U}_{j,l}$ is constructed by combining radial window W and angular window V and is expressed as

$$\tilde{U}_{j,l}(w) = W_j(w) V_j(S_{\theta_l} w) \tag{4}$$

Where, the angle θ_l have same slope but are not equally spaced. S_θ is shear matrix,

$S_\theta = \begin{pmatrix} 1 & 0 \\ \tan\theta & 1 \end{pmatrix}$. Shear matrix S_θ is used to maintain the symmetry around the origin and rotation by $\pm\prod/2$ radiance. The family $\tilde{U}_{j,l}$ implies a concentric tiling whose geometry is shown in Figure 2. The shaded region represents a wedge.

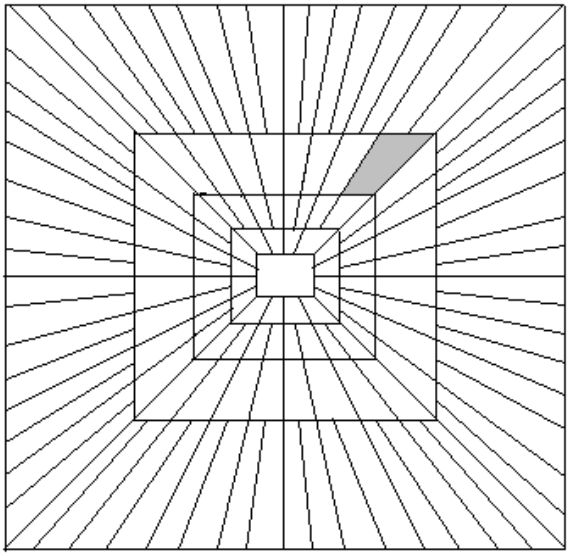

FIGURE 2: Basic digital tiling.

The above construction gives pseudopolar tiling, an alternative to ideal polar tiling. In FDCT via wrapping the curvelets at a wedge are wrapped for a given scale and angle by translating the curvelets on regular rectangular grid which is same for every angle within each quadrent with proper orientation. The frequency domain definition of digital curvelet is,

$$\overline{\varphi^D_{j,l,k}}[t_1,t_2] = \hat{U}_j[t_1,t_2]e^{-i2\Pi[k_1t_1+k_2t_2]} \tag{5}$$

where, $\hat{U}_j[t_1,t_2]$ is Cartesian window. Here the discrete localizing window $\hat{U}_{j,l}[n_1,n_2]$ does not fit in a rectangle, aligned with axes. At each scale j, there exist two constants $L_{1,j} \approx 2^j$ and $L_{2,j} \approx 2^{j/2}$ such that for every orientation θ_l, one can tile the two-dimensional plane which translates the respective rectangle by multiples of $L_{1,j}$ in the horizontal direction and $L_{2,j}$ in the vertical direction. The windowed data is wrapped around the origin. The correspondence between the wrapped and original indices is one to one where the wrapping transformation is reindexing of the data. Figure 3 illustrates the wrapping process.

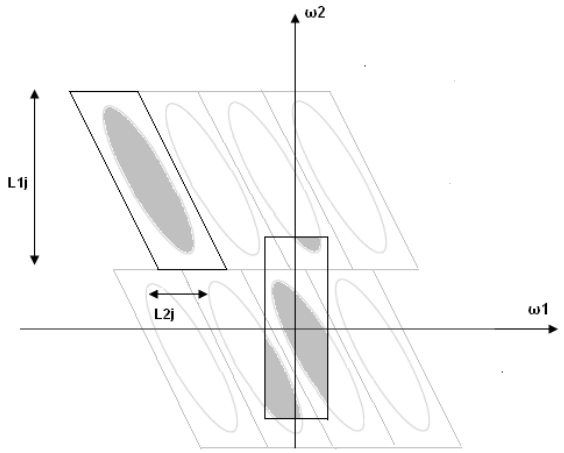

FIGURE 3: Illustrate the wrapping process

Discrete Curvelet transform is expressed as

$$c^D(j,l,k) = \sum_{0 \le t_1, t_2 < n} f[t_1, t_2] \overline{\varphi^D_{j,l,k}[t_1, t_2]} \quad (6)$$

where, $c^D(j,l,k)$ represents curvelet coefficients with *j* as scale parameter, *l* as orientation parameter and *k* as position parameter. $f[t_1, t_2]$ is an input of Cartesian arrays [16]. This transform is also invertible. To illustrate the FDCT decomposition, a standard Lena image is decomposed at three levels with eight orientations as shown in Figure 4. The coarser first level FDCT coefficients are low frequency components and are wavelet coefficients because they do not have orientation. Second finer scale gives eight different oriented wedges where as the third finest scale gives sixteen corresponding oriented wedges. The number of wedges in a subband increases by a factor of two only after every other scale. Here FDCT via wrapping is used as it is simple to implement.

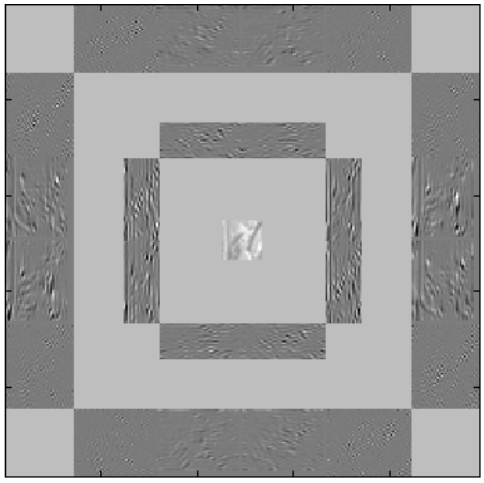

FIGURE 4: Decomposition Lena image at two scale with eight directions in FDCT domain

4. LEARNING FAST DISCRETE CURVELET COEFFICIENTS

The decomposition of input image in Fast Discrete Curvelet Transform (FDCT) domain gives coarser scale coefficients and finer scale coefficients. The coarser scale subband contains low frequency components which are wavelet components as they do not have orientation. The finer scale subbands contain directional high frequency components. The high frequency components at finer scale of low resolution test image are estimated by learning them from high resolution training images in dataset. The learning procedure is performed by finding the minimum Euclidean distance between coefficients of low-resolution test image and all high-resolution training images in particular subband. This gives best closeness of the coefficients. To represent an image fine edges are important. In this proposed work 4x4 pixel block is considered as edge primitive element localized in low-resolution test image and the corresponding 8x8 pixel block in the high resolution image. The low resolution test image is decomposed at two levels and all the training images in data set are decomposed at three levels in FDCT domain. The size of the test image is of MxM pixel where as all training images are of 2Mx2M size. Figure 5 illustrates the learning of fast discrete curvelet coefficients at the finer scale from a set of N training images.

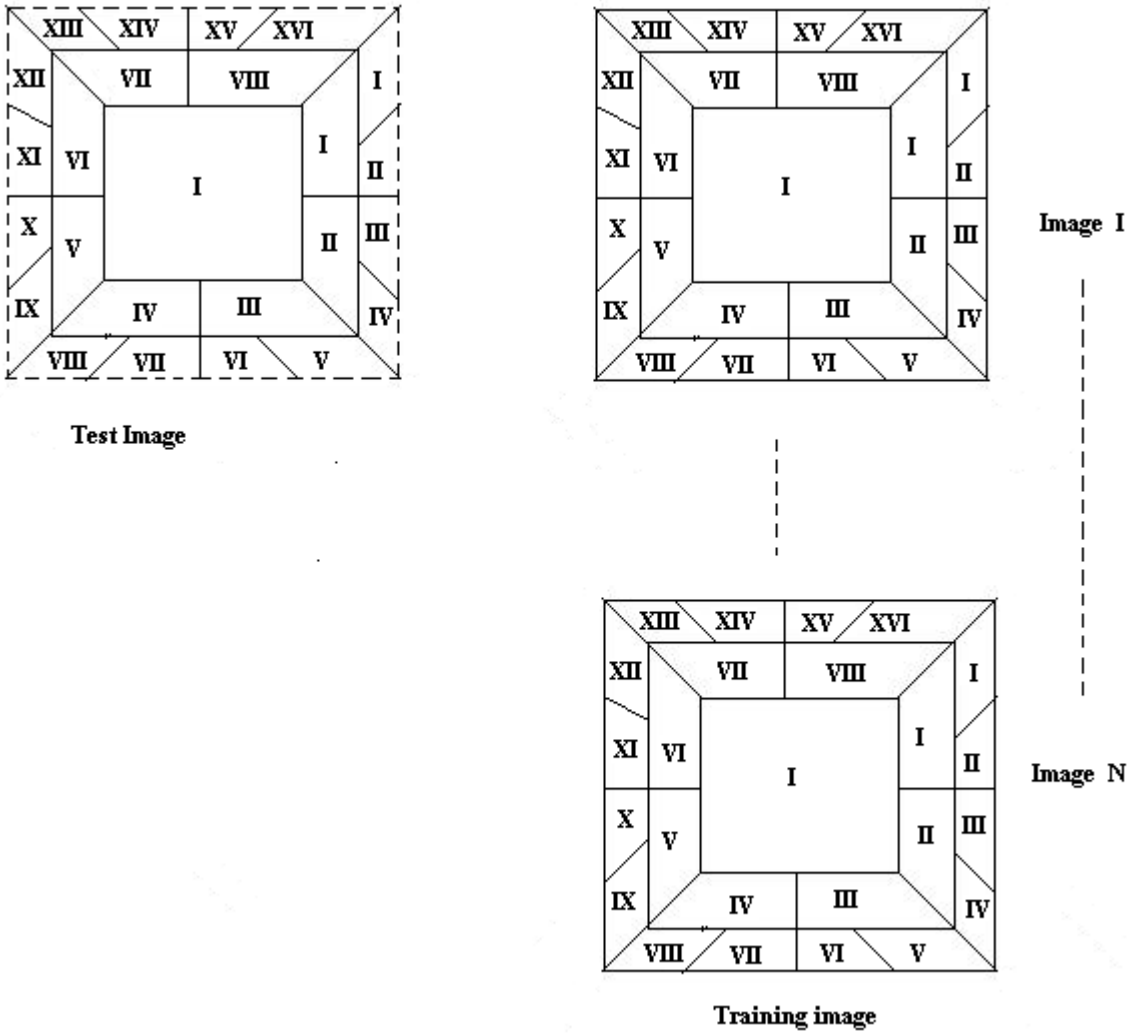

FIGURE 5: Illustrates the learning process in FDCT domain

The minimum Euclidean distance is computed by comparing low-resolution test image edge primitive element with corresponding high-resolution training images at second coarser scale. The minimum Euclidean distance gives best match of edge primitive element. The finer scale

coefficients of low-resolution test image at particular subband are learnt from the corresponding third scale coefficients of high-resolution training images in dataset. Zero tree concept is applied to learn the curvelet coefficients at finer scale of the low-resolution test image. To find the best match, minimum Euclidean distance of curvelet coefficients at *I-VIII* subbands of low-resolution test image and the corresponding subbands of the high-resolution training images are considered. The location (l,k) as $d(l,k)$ at *I-VIII* subbands of the test image is searched for best match in all the training images in particular subband. The best matched curvelet coefficients at the finest scale of a training image for the given location are copied to the corresponding subbands *I-XVI* of low-resolution test image. The formula used to calculate the minimum Euclidean distance is as follows:

$$m(\hat{p},\hat{q}) = \arg\min_{m,p,q} sqrt[\left|d_{IS2}(l,k) - d_{I(m)S2}(p,q)\right|^2 + \left|d_{IIS2}(l,k) - d_{II(m)S2}(p,q)\right|^2$$
$$+ \left|d_{IIIS2}(l,k) - d_{III(m)S2}(p,q)\right|^2 + \left|d_{IVS2}(l,k) - d_{IV(m)S2}(p,q)\right|^2 + \left|d_{VS2}(l,k) - d_{V(m)S2}(p,q)\right|^2$$
$$+ \left|d_{VIS2}(l,k) - d_{VIS2}(p,q)\right|^2 + \left|d_{VIIS2}(l,k) - d_{VII(m)S2}(p,q)\right|^2 + \left|d_{VIIIS2}(l,k) - d_{VIII(m)S2}(p,q)\right|^2] \quad (7)$$

Here $d_J(m)S$ denotes the curvelet coefficients for the *m*th training image at the J th subband, at scale *S* and *m=1, 2….K*. The best match of the test image at (l,k) th location is $(\hat{p},\hat{q})$ th location of m th training image at scale S . The best match of 8x8 pixel area is copied at the corresponding subbands of the test image. So the 8x8 pixel area in the low resolution test image is learnt from different training images independently. When 4x4 block at second level does not find a good match in the training data set minimum distance is too large. It shows that high resolution representation is not available in the dataset which introduces artifacts in the reconstructed image. Such artifacts can be avoided by choosing certain threshold for minimum distance. First scale curvelet coefficients are lowpass coefficients and are not considered while calculating minimum Euclidean distance.

The learning algorithm is given in steps as below:

1) Perform two-level FDCT decomposition on the low-resolution test image of size MxM.
2) Perform three-level FDCT decomposition on all the training images each of size 2Mx2M.
3) Find minimum Euclidean distance by considering 4x4 pixel block of curvelet coefficients in subbands *I-VIII* at second level of low resolution test image and all high resolution images in training data set.
4) If minimum Euclidean distance < threshold, copy 8x8 block of curvelet coefficients in subband *I-XVI* of high resolution training image at third level to the corresponding *I-XVI* subband of low-resolution test image else set them zero.
5) Repeat steps 3-4 for every 4x4 block of curvelet coefficients in *I-VIII* subbands at second level of low resolution image.
6) Perform inverse FDCT transform to obtain the high-resolution image of the given test image.

In post processing histogram specification technique is used for image enhancement. The finest level curvelet coefficients of the low resolution test image are learnt from the high-resolution training images in dataset. In SR, during upsampling process edges get blurred. The edge primitive element is used to learn the LR edge from its HR representation locally. Here 4x4 pixel block is selected as edge primitive element in the LR image and the corresponding 8x8 pixel area in the HR image. Each local region is learned independently from HR data set. This edge primitive gives the localization in the particular subband of the image. Large edge primitive gives

poor localization and better matching where as small edge primitive gives better localization but more fails matching.

5. EXPERIMENTAL RESULTS

Experiments are carried out on different types of images to find the efficiency of the proposed algorithm. Arbitrary high resolution gray images of different objects are downloaded from the internet to form the training data set. The training images in the data set considered are of 100. A high resolution gray image which does not belong to training data set is considered to obtain a low resolution image. This low resolution image is obtained through imaging model and upsampled to obtain a super-resolution image. Figure 6 (a) shows a low-resolution image of old man and Figure 6 (b) is high resolution image. Bicubic interpolated image is shown in Figure 6(c). The interpolated image is blurred one and cannot get the details of eye and lines on the forehead. The image shown in Figure 6 (d) is super-resolved by using Contourlet transform. The image shows the fine details of the eye and the lines on the forehead face. Image shown in Figure 6(e) is super-resolved by proposed method. The super-resolved image shows every detail of the eyes, lines on the forehead and face. The details of the eye brows can be visualized in the image and image is sharp.

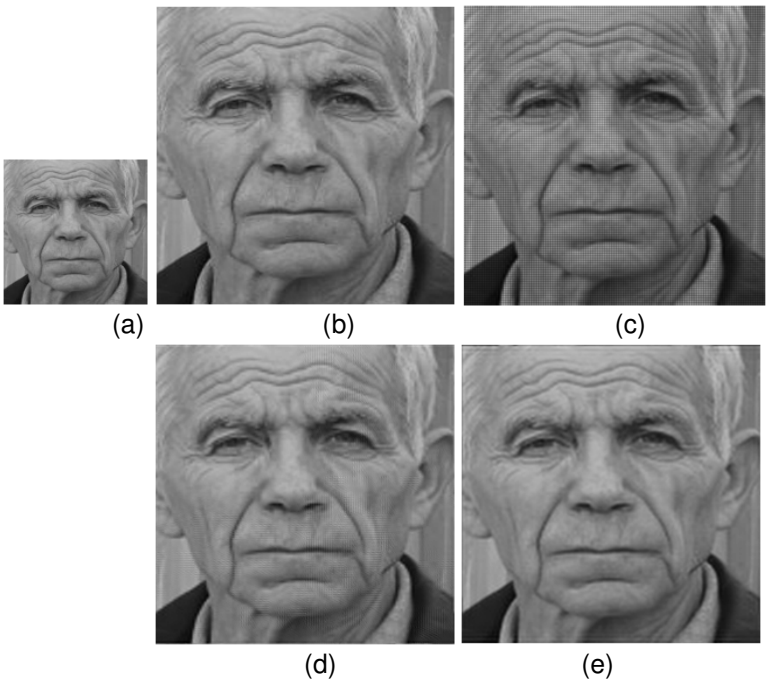

FIGURE 6: a) Low resolution image b) Original High resolution image c) Bicubic interpolated image d) Super-resolved image by using Contourlet transform e) Super-resolved image by using proposed method.

Image shown in Figure 7 (a) is low resolution image of a girl and original high resolution image is shown in figure 7(b). Image shown in figure 7(c) is bicubic interpolated image which is blurred one. The details of texture on the transparent hat and, the shadow on the face appear to be blurred. The details of eye have lost and the hairs found to be total undistinguishable. Figure 7 (d) shows the super-resolved image by using Contourlet transform. The texture on hat, shadow on face and the details of eyes are sharp and details have been retained. Image shown in figure 7(e) is of the proposed method. The particulars of the texture on hat have been reconstructed without blur. Black Strips on the hat have been reconstructed without blur and edge of hat is artifact free. The details of the eye balls and eye brow can be observed clearly. The hair strands can be distinguishable. Image looks sharper.Image shown in figure 8(a) is of low resolution Barbara image, cropped from the original image and figure 8(b) is the high resolution version of it. Bicubic interpolated image is shown in figure 8(c) where the blurred image have been observed at edges.

Strips on scarf appeared to be blurred. Image shown in figure 8(d) is super-resolved by using the Contourlet transform. Image shows sharp strips on the scarf with minor details on palm and, image is not blurred. The image shown in figure 8(e) is of proposed method. Here every strip on the scarf is distinguishable and has been reconstructed well. The texture is retained in the reconstructed image without blur. Details on palm are visible and image is sharper.

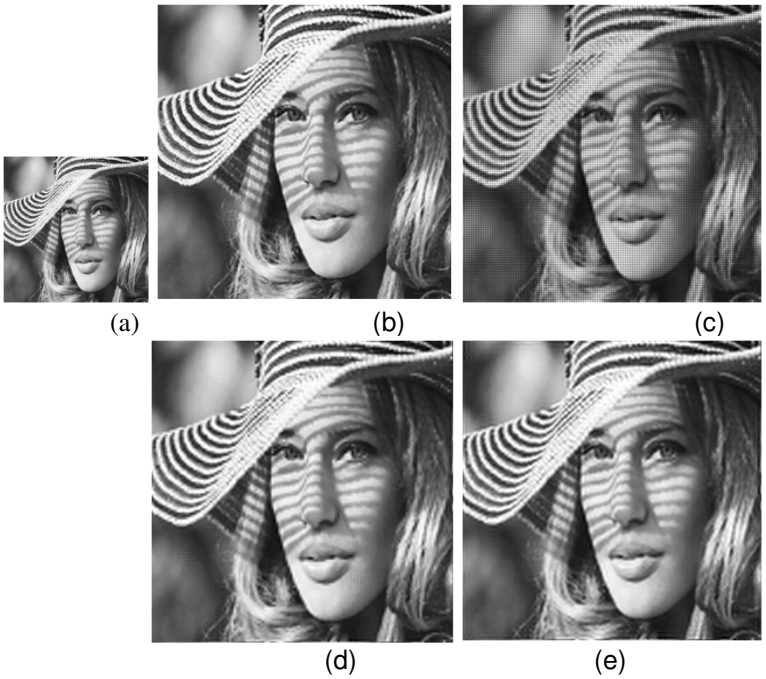

FIGURE 7: a) Low resolution image b) Original High resolution image c) Bicubic interpolated image d) Super-resolved image by using Contourlet transform e) Super-resolved image by using proposed method

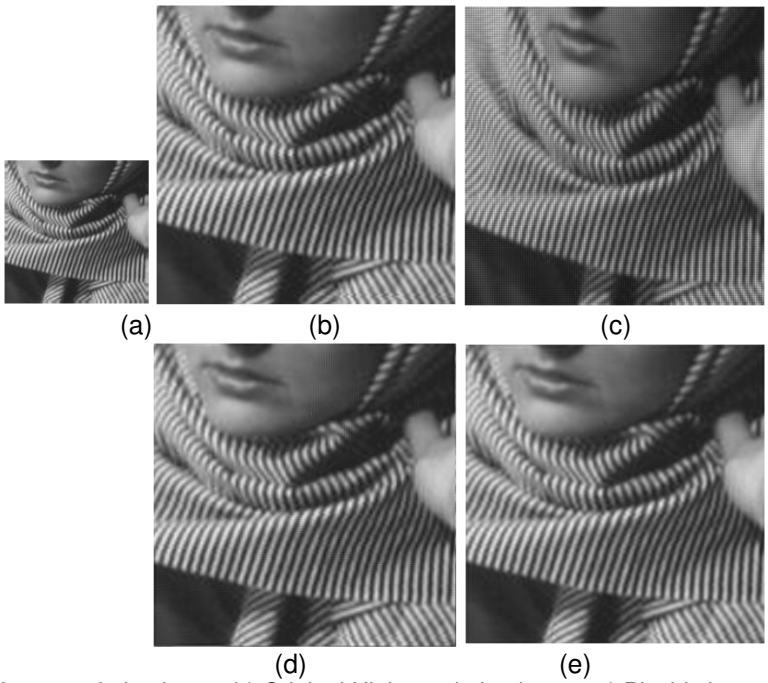

FIGURE 8: a) Low resolution image b) Original High resolution image c) Bicubic interpolated image d) Super-resolved image by using Contourlet transform e) Super-resolved image by using proposed method.

The reconstructed image is analyzed by computing mean squared error (MSE), peak signal-to-noise ratio (PSNR) in db and correlation coefficient (CC). Table 1 shows the comparison of the proposed method over bicubic interpolation and Contourlet learning algorithm for gray images.

Image	MSE			PSNR			Correlation		
	Bicubic	Contourlet Learning	Proposed Method	Bicubic	Contourlet Learning	Proposed Method	Bicubic	Contourlet learning	Proposed method
Old Man	0.0361	0.0026	0.0016	20.3618	31.8079	33.7574	0.8950	0.9815	0.9882
Girl	0.0472	0.0151	0.0137	18.2783	23.2210	23.6505	0.9333	0.9630	0.9675
Barbara	0.0443	0.0113	0.0095	19.9407	26.3643	27.1431	0.9283	0.9677	0.9729

TABLE 1: Comparison of MSE, PSNR in db and correlation coefficient.

Experiments on color images also have been conducted to recognize the performance of the proposed method. The training data set of high quality 100 color images is considered for the experimentation. The low resolution image is obtained from the same imaging model and it does not belong to data set. The input low resolution and all the high resolution images from data set are converted into $Y - C_b - C_r$ format. The Y plane which represents luminance is used to learn the curvelet coefficients of low resolution image. The other two planes C_b and C_r are interpolated with bicubic interpolation. The high resolution image is then reconstructed by combining these three planes.

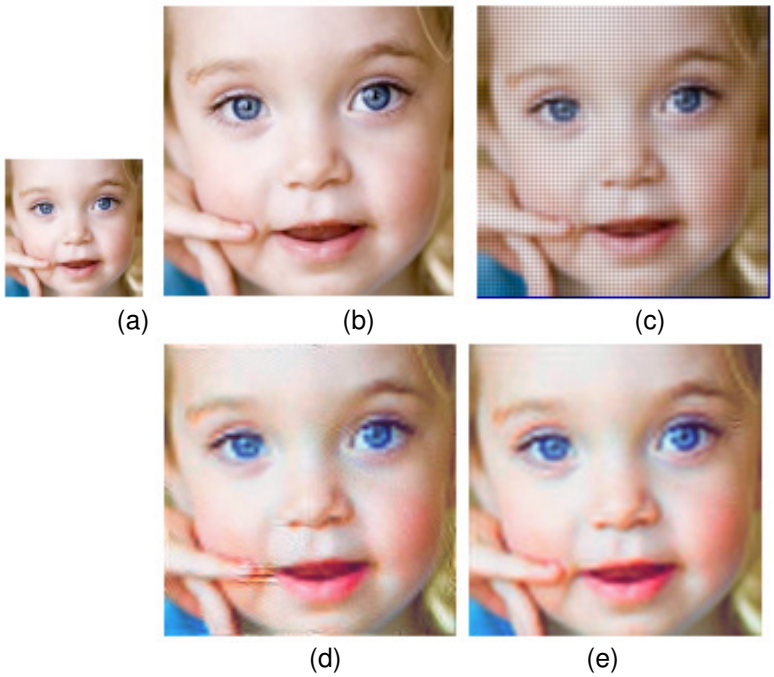

FIGURE 9: a) Low resolution image b) Original High resolution image c) Bicubic interpolated image d) Super-resolved image by using Contourlet transform e) Super-resolved image by using proposed technique

Figure 9 (a) shows the low resolution image of a child and figure 9(b) is its high resolution version. The image shown in figure 9(c) is bicubic interpolated image. The result shows blurred

image with less details. Figure shown in 9(d) is super-resolved image by using Contourlet transform. The reconstructed image shows more details such as eyes, eye balls and eye brows. The image shown in figure 9(e) is super-resolved by the proposed method. All the details of eye and eye brow have been preserved in the reconstructed image without blur.Figure 10 (a) shows the low resolution image of face and figure 10(b) is original high resolution image. The image shown in figure 10(c) is bicubic interpolated image. The result shows blurred image with few details. Image shown in figure 10(d) is super-resolved by using Contourlet transform. Almost all the details are visible and the image is sharp. The image shown in figure 10 (e) is super-resolved by proposed method. The result shows sharp image with all details such as eye balls, eye brow. The eyelids are also visible clearly.

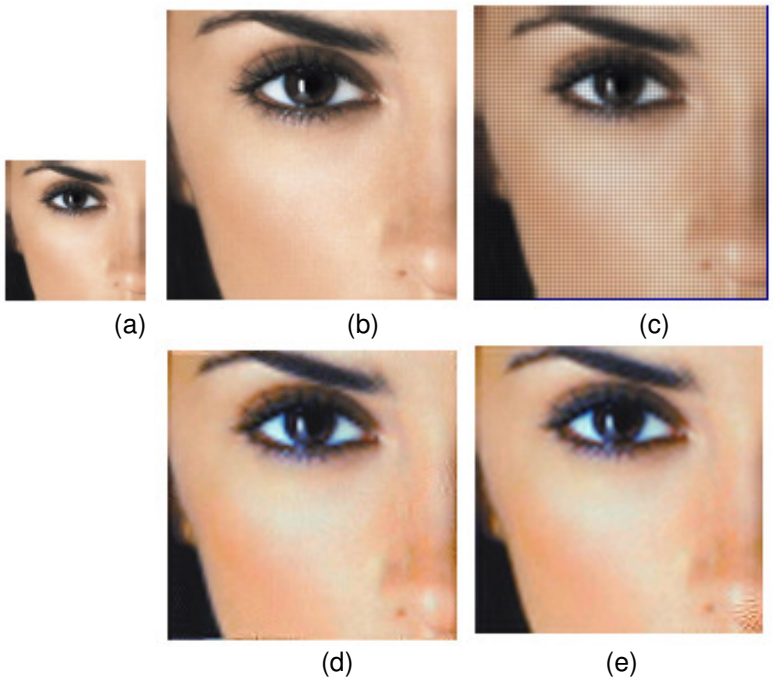

FIGURE 10: a) Low resolution image b) Original High resolution image c) Bicubic interpolated image d) Super-resolved image by using Contourlet transform e) Super-resolved image by using proposed technique

Table 2 shows the comparison of the proposed method over bicubic interpolation and Contourlet transform algorithm for color images in terms of MSE and PSNR in db. The mean squared error between the original image and reconstructed super-resolved image is expressed as:

$$MSE = \frac{\sum_{a,b}\left(S(a,b) - \hat{S}(a,b)\right)^2}{\sum_{a,b}\left(S(a,b)\right)^2} \tag{8}$$

Where $S(a,b)$ original high resolution image and $\hat{S}(a,b)$ is reconstructed super resolved image. The peak signal to noise ratio in db is defined as:

$$PSNR = 10\log\left(\frac{255\text{^}2}{MSE}\right) \tag{9}$$

Correlation coefficient between original high-resolution image and reconstructed super-resolved image is computed as

$$r = \frac{\sum_m \sum_n \left(A_{mn} - \overline{A}\right)\left(B_{mn} - \overline{B}\right)}{\sqrt{\left(\sum_m \sum_n \left(A_{mn} - \overline{A}\right)^2\right)\left(\sum_m \sum_n \left(B_{mn} - \overline{B}\right)^2\right)}} \tag{10}$$

where $\overline{A} = mean(A)$, and $\overline{B} = mean(B)$

Image	MSE			PSNR		
	Bicubic	Contourlet Learning	Proposed method	Bicubic	Contourlet Learning	Proposed Method
Child	0.0225	0.0053	0.0049	19.2070	25.5049	25.8248
Face	0.0213	0.0038	0.0030	20.0667	27.5502	28.5381

TABLE 2: Comparison of MSE and PSNR in db

For all the images there is appropriate improvement in the MSE, PSNR and correlation coefficient. The PSNR of the proposed method for the textured image has been improved almost by 6 db over bicubic interpolation and almost 1% improvement over the Contourlet learning method has been observed. An appropriate improvement in correlation coefficient is also observed with the proposed method.

6. CONCLUSION

The super-resolved image is reconstructed by estimating the finer scale FDCT coefficients of low-resolution test image by learning them from a set of high resolution training images. In this proposed method, FDCT captures the smoothness along the curves and high-resolution edges are learned from a training set at multiresolution level. This technique is useful when a single observation is available. The reconstructed result depends upon the high-resolution training images in dataset and the method is resolution dependent. Bicubic interpolation technique gives blurred reconstructed images whereas compatible results have been observed for Contourlet learning method. The appropriate improvement in MSE, PSNR and correlation coefficient is observed with the proposed method. Computational complexity is less than Contourlet learning method.

7. REFERENCES

[1] R.Y.Tsai and T.S.Hung, "Multiframe image restoration and registration," in Advances in Computer Vision and Image Processing,vol.1,chapter 7,pp.317-339.JAI press,greenwich,Conn,USA,1984.

[2] M.Irani and S. Peleg." Improving resolution by image registration," CVGIP: Graphical Models and Image Processing, vol. 53, no. 3 pp. 231-239, 1991.

[3] M. Irani and S. Peleg," Motion analysis for image enhancement: resolution, occlusion, and transparency," Journal of Visual Communication and Image Representation, vol. 4, no. 4, pp. 324-335,1993.

[4] M. K. Ng, J. Koo, and N. K. Bose." Constraintet total least-sqeuare nsorcomputations for high-resolution image reconstruction with multisensors," International Journal Of Imaging Systems and Technology, vol. 12, no. 1, pp. 35-42, 2002.

[5] M. K. Ng and N. K. Bose," Analysis of displacement errors in high-resolution image reconstruction with multisensors," IEEE Transactions on Circuits and Systems Part I, vol. 49, no. 6, pp. 806-813,2002.

[6] N. Nguyen, P. Milanfar, and G. Golub," A computationally efficient super-resolution image reconstruction algorithm," IEEE transaction on Image Processing, vol. 10, no. 4, pp. 573-583, 2001

[7] R.R. Schuitz and R. L. Stevenson," A Bayesian approach to image expansion for improved definition," IEEE Transactions on Image Processing, vol. 3, no. 3, pp. 233-242,1994

[8] D. Rajan and S.Chaudhuri," An MRF-based approach to generation of super-resolution images from blurred observations," Journal of mathematical Imaging and Vision, vol. 16, no. 1, pp. 5-15, 2002.

[9] D. Rajan and S. Chaudhuri," Simultaneous estimation of super-resolved scene and depth map from low resolution defocused observations," IEEE transctions on Pattern Analysis and Machine Intelligance, vol. 25,no. 9, pp. 1102-1117, 2003

[10] M. Elad and A. Feuer," Restoration of a single super-resolution image from several blurred, noisy and under sampled measured images," IEEE transactions on Image Processing, vol. 6. no.12. pp. 1646-1658, 1997

[11] S. Baker and T. Kanade," Limits on super-resolution and how to break them," IEEE Transactions on Pattern Analysis and Machine Intelligence, vol. 24, no. 9, pp. 1167-1183, 2002

[12] D. Capel and A. Zisserman," Super-resolution from multiple views using learnt image models," In Proceedings of IEEE Computer Society Conference on Computer Vision and pattern Recognition (CVPR'01), vol. 2, pp. II-627-II-634, Kauai, Hawaii, USA, December 2001

[13] W. T. Freeman, T. R. Jones, and E. C. pasztor," Example-based super-resolution," IEEE Computer Graphics and Applications, vol. 22, no. 2, pp. 56-65, 2002

[14] M.V. Joshi and S. Chaudhuri," Alearning-based method for image super-resolution from zoomed observations," In Proceedings of 5th International Conference on Advances In Pattern Recognition (ICAPR'03), pp. 179-182, Culcutta, India, December 2003

[15] C.V. Jiji, M. V. Joshi, and S. Chaudhuri," Single –frame image super-resolution using learned wavelet coefficients," International Journal of Imaging Systems and Technology, vol. 14, no. 3, pp. 105-112,2004

[16] H. Chang, D. Y. Yeung, and Y. Xiong," Super-resolution trough neighbor embedding," in Proceedings of IEEE Computer Society Conference on Computer Vision and Pattern Recognition (CVPR'04), vol.1, pp. I-275-I-282, Washington, DC, USA, June-July 2004.

[17] J. S. Park and S. W. Lee." Enhancing low-resolution facial images using error back-projection for human identification at a distance," in Proceedings of 17th IEEE International Conference on Pattern Recognition (ICPR'04), vol.1, pp. 346-349, Cambridge, UK, August 2004

[18] J.Sun, N. N. Zheng, H. Tao, and H. Y. Shum," image hallucination with primal sketch priors," In Proceedings of IEEE Computer Society Conference on Computer Vision and Pattern Recognition (CVPR'03), vol. 2, pp. II-729-II-736, Madison, Wis, USA, June 2003

[19] M.N. Do and M. Vetterli," The contourlet transform: an efficient directional multiresolution image representation," IEEE transactions on Image Processing, vol. 14, no. 12, pp. 2091-2106, 2005

[20] C.V.Jiji and S.Chaudhuri, "Single-frame image Super-resolution through Contourlet Learning,"EURASIP Jounal on Applied Signal Processing ,vol.2006, Article ID 73767,pp.1-11,2006

[21] D. Glasner, S. Bagon, and M. Irani," Super-resolution from a single image," IEEE International Conference on Computer Vision (ICCV), pp. 349-356,2009

[22] P. P. Gajjar and M. V. Joshi," New learning based super-resolution use of DWT and IGMRF prior," IEEE Transactions on Image Processing, vol. 19, no. 5, pp. 1201-1213, May 2010.

[23] C. Kim, K. Choi, H. Lee, K. Hwang, and J. B. Ra," Robust Learning-Based Supre-resolution," in Proceedings of International Conference on Image Processing (ICIP'10), pp. 2017-2020, Hong Kong, Sept. 2010.

[24] K. I. Kim and Y. Kwon," Sinlge-image Super-Resolution Using Spsrse regression and Natural Image prior," IEEE Transcation on Pattern Analysis and Machine Intelligence, vol. 32, no. 6, pp. 1127-1133, 2010.

[25] E. J. Candes and D. L. Donoho," New tight frames of curvelets and optimal representations of objects with piecewise-C^2 singularities," Comm. on Pure and Appl. Math. Vol.57, pp. 219–266, 2004.

[26] E.J.Candes, D.L.Donoho and L.Ying," Fast Discrete Curvelet Transform.," Journal of Multiscale modeling & simulation, vol.5, no.3, pp.861—899, 2006.